special communication

Three-dimensional reconstruction of human diaphragm with the use of spiral computed tomography

NICOLAS PETTIAUX,[1] MARIE CASSART,[2] MANUEL PAIVA,[1] AND MARC ESTENNE[3]
[1]*Biomedical Physics Laboratory,* [2]*Department of Radiology, and* [3]*Department of Chest Medicine, Erasme University Hospital, Université Libre de Bruxelles, B-1070 Brussels, Belgium*

Pettiaux, Nicolas, Marie Cassart, Manuel Paiva, and Marc Estenne. Three-dimensional reconstruction of human diaphragm with the use of spiral computed tomography. *J. Appl. Physiol.* 82(3): 998–1002, 1997.—We developed a technique of diaphragm imaging by using spiral computed tomography, and we studied four normal subjects who had been previously investigated with magnetic resonance imaging (A. P. Gauthier, S. Verbanck, M. Estenne, C. Segebarth, P. T. Macklem, and M. Paiva. *J. Appl. Physiol.* 76: 495–506, 1994). One acquisition of 15- to 25-s duration was performed at residual volume, functional residual capacity, functional residual capacity plus one-half inspiratory capacity, and total lung capacity with the subject holding his breath and relaxing. From these acquisitions, 20 coronal and 30 sagittal images were reconstructed at each lung volume; on each image, diaphragm contour in the zone of apposition and in the dome was digitized with the software Osiris, and the digitized silhouettes were used for three-dimensional reconstruction with Matlab. Values of length and surface area for the diaphragm, the dome, and the zone of apposition were very similar to those obtained with magnetic resonance imaging. We conclude that satisfactory three-dimensional reconstruction of the in vivo diaphragm may be obtained with spiral computed tomography, allowing accurate measurements of muscle length, surface area, and shape.

respiratory muscles; chest wall; mechanics of breathing

IN PATIENTS with chronic obstructive pulmonary disease (COPD), hyperinflation of the lungs may impair the inspiratory function of the diaphragm by decreasing its operating length, altering its shape, and changing its mechanical coupling with the lower rib cage. Understanding how hyperinflation affects diaphragm function, therefore, requires information on the three-dimensional (3D) shape of the muscle with measurements of its lung-apposed and rib cage-apposed length and surface area.

In two previous studies from our laboratory, we have used magnetic resonance imaging (MRI) in normal subjects to study the 3D shape of the diaphragm at functional residual capacity (FRC) (3) and at different lung volumes (1). Although this technique proved to be well suited for the study of subjects with normal pulmonary function, preliminary experiments showed that it was not adequate for the study of patients with COPD. Indeed, to obtain a satisfactory resolution, repeated acquisitions with prolonged breath holds had to be performed at each volume studied (1, 3), making the procedure long and demanding to the subject. Application of this technique to patients with severe COPD proved to be impossible, with most patients being unable to sustain the breath holds.

We decided, therefore, to develop a more convenient technique of diaphragm imaging by using spiral computed tomography (CT). With this technique, a predefined region is scanned continuously at constant table feed rate, allowing subsequent reconstruction of individual slices anywhere within the spiral volume range. In this study, we describe the spiral CT technique, report results obtained in four normal subjects at different lung volumes, and compare these results with those previously obtained in the same subjects with MRI. In addition, we provide details on the computerized method used to handle the data.

MATERIALS AND METHODS

Subjects, CT instrument, and measurements. We studied the four normal men who had been previously studied by Gauthier et al. (1). Details on the subjects are given in Table 1. All were highly trained in respiratory maneuvers. With the subject lying supine, we fixed a metal wire around the costal margin to identify the loci of origin of the costal diaphragmatic fibers. A metal bullet was also fixed on the xiphoid process and was used as a reference point.

We used spiral CT, the acquisitions being obtained on a Somatom Plus 4A (Siemens, Erlangen, Germany) set to the following conditions: 8-mm slice thickness, 10 mm/s table speed, 140 kV, 200 mA, 1-s rotation time. We carried out the acquisitions at residual volume (RV), FRC, total lung capacity (TLC), and FRC plus one-half inspiratory capacity (FRC+). To attain this last volume, the subjects were connected to a spirometer and instructed to breathe in to TLC and slowly expire until FRC+ was reached. At each volume, the subjects were asked to hold their breath and to relax against a closed glottis. The estimated total irradiation dose was 48.4 mGy.

Before the spiral acquisition, a frontal view of the chest wall was obtained at each lung volume; it was used to define the acquisition range, which extended from 1 cm above the diaphragmatic dome to 1 cm below the metal wire at the costal margin. The acquisition time ranged from 15 to 25 s according to the volume studied and the height of the subject.

At each volume, we reconstructed 8-mm-thick axial (transverse) slices every 5 mm (overlapping each other by 3 mm). On the axial slice that included the xiphoid marker, we then defined 20 coronal and 30 sagittal reconstructions. In the coronal plane, images were reconstructed between the xi-

0161-7567/97 $5.00 Copyright © 1997 the American Physiological Society

Downloaded from www.physiology.org/journal/jappl by ${individualUser.givenNames} ${individualUser.surname} (095.085.069.063) on November 26, 2018.
Copyright © 1997 the American Physiological Society. All rights reserved.

Table 1. *Details of subjects studied*

Subject No.	Age, yr	Weight, kg	Height, cm
S1	40	65	173
S2	40	65	180
S3	53	70	172
S4	44	76	192

phoid marker anteriorly and the outer aspect of the rib cage posteriorly; in the sagittal plane, images were reconstructed between the lateral aspects of the rib cage, with the midsagittal slice crossing the xiphoid marker. Knowing the distance between the two extreme slices and the number of reconstructions in each plane, we were then able to precisely position each reconstructed slice relative to the reference point.

3D reconstruction. We transfered 350–384 reconstructed images for each subject from the workstation of the CT to a Pentium personal computer on which they were sorted accord-

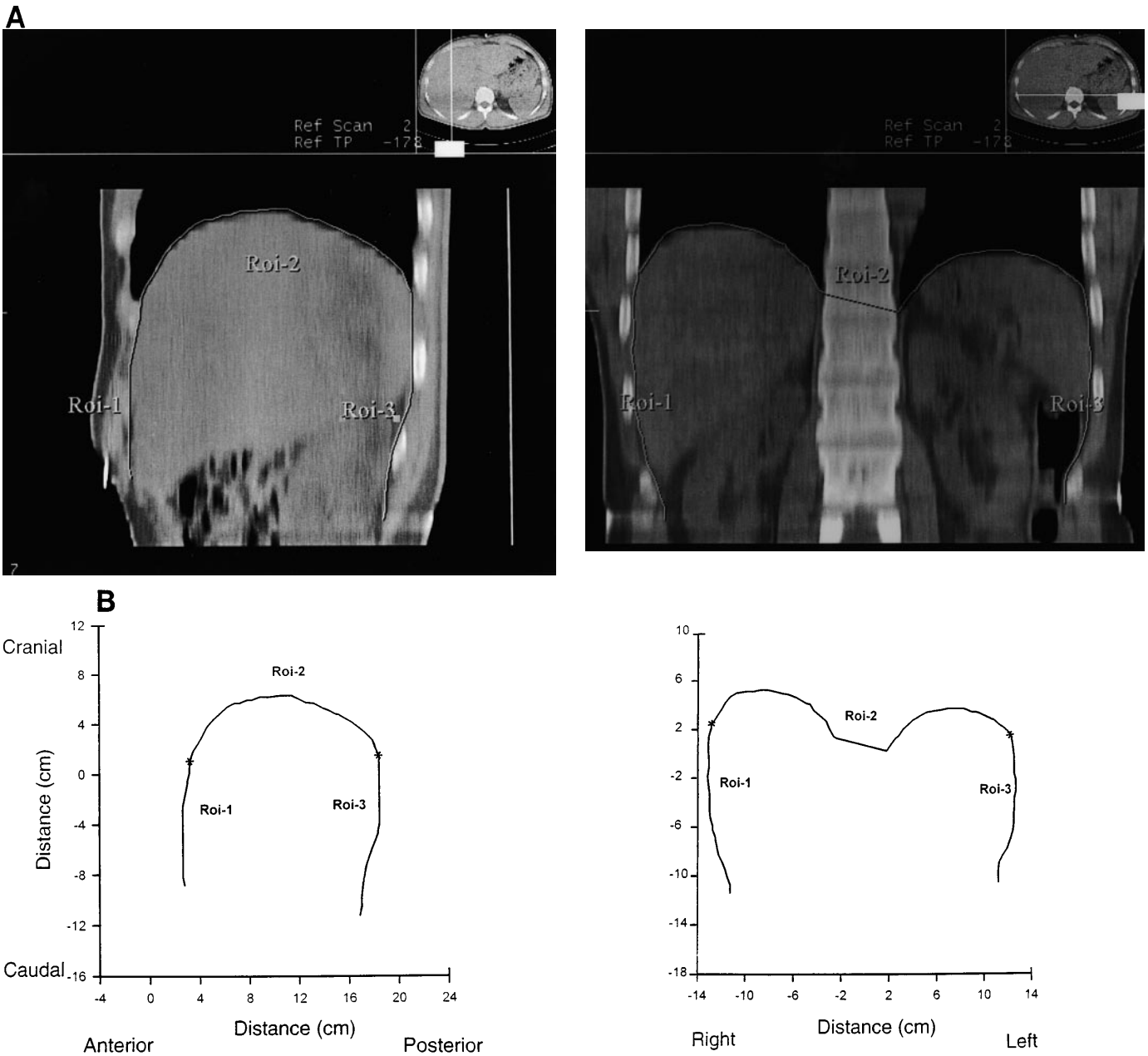

Fig. 1. *A*: representative sagittal (*left*) and coronal (*right*) reconstructed computed tomography images obtained in *subject S2* at functional residual capacity. Images digitized with Osiris are shown as displayed on the personal computer screen; *insets*, axial slice shows location of reconstructed sagittal and coronal images. *B*: corresponding digitized diaphragm silhouettes. *, Location of costophrenic angles. Region of interest (ROI) 1 corresponded to diaphragm apposed (i.e., zone of apposition) to anterior and right aspects of rib cage; ROI 3 corresponded to diaphragm apposed to posterior and left aspects of rib cage; ROIs 1–3 extended from costal margin marker to costophrenic angle; ROI-2 corresponded to diaphragm apposed to lungs (i.e., diaphragm dome) and extended between right and left (coronal view) or anterior and posterior (sagittal view) costophrenic angles. Ref, reference; TP, transverse plane.

Downloaded from www.physiology.org/journal/jappl by ${individualUser.givenNames} ${individualUser.surname} (095.085.069.063) on November 26, 2018.
Copyright © 1997 the American Physiological Society. All rights reserved.

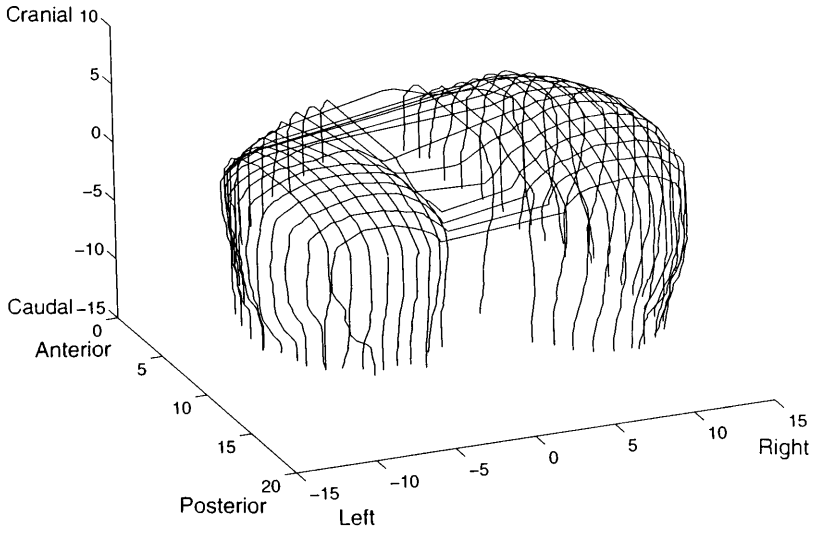

Fig. 2. Three-dimensional reconstruction of diaphragm in *subject S2* at functional residual capacity. Reconstruction is shown from posterior-superior left lateral perspective.

ing to their orientation and the volume studied. The files were then handled by a single investigator (*MC*) by using a locally adapted version of the software Osiris that has been developed at the University Hospital of Geneva to analyze radiological data (2, 4).

On each slice, the contour of the diaphragm was digitized in three contiguous segments [region of interest (ROI)] that corresponded to the zone of apposition (ROI-1 and ROI-3 in Fig. 1) and the dome (ROI-2 in Fig. 1). The caudal boundary of the zone of apposition was defined by the position of the costal marker, and the cranial boundary of the zone of apposition was defined by the costophrenic angle located at the time of digitization. On the coronal views, ROI-1 and ROI-3 corresponded to the right and left portions of the zone of apposition (Fig. 1, *right*); on the sagittal views, ROI-1 and ROI-3 corresponded to the anterior and posterior portions of the zone of apposition (Fig. 1, *left*).

We discarded ~6 coronal and ~10 sagittal images at each lung volume because they showed unclear diaphragm silhouettes in the region of the mediastinum or because they intercepted with the thoracic wall. Therefore, a total of ~14 coronal and ~20 sagittal images were used at each lung volume for 3D reconstruction. In some of these images, a limited portion of the diaphragm dome was ill defined because of the presence of the heart/mediastinum; this portion was reconstructed by linear interpolation between the closest well-defined points of diaphragm contour.

The following variables were exported from Osiris to a software written in Matlab (5): the coordinates of each digitized ROI with the number of its slice and the coordinates of the xiphoid reference marker. These data and the information provided by the CT (i.e., the distance between the 2 extreme reconstructed slices and the number of slices in each plane, and the number of the slice crossing the reference point) were used for 3D reconstruction (Fig. 2).

Length and surface measurements. Total diaphragm length (L_{di}), the length of the zone of apposition (L_{ap}), and the length of the dome (L_{do}) were directly measured on the midcoronal silhouettes and on the largest sagittal silhouettes in the middle of the right or left dome. We elected to restrict measurements of muscle length to these slices because the direction of the muscle fibers, which radiate from the central tendon, should not be too different from these planes.

To calculate the surface area of the diaphragm from the 3D reconstructions, we created small triangular surfaces that joined two points from one ROI with one point on the adjacent ROI. The surface areas of the dome (A_{do}) and of the zone of apposition (A_{ap}) were calculated as the sum of the surface areas of these triangles, and total diaphragmatic area (A_{di}) was obtained by summation of A_{do} and A_{ap}. A_{do} was measured by using triangular surfaces created between ROIs 2 of adjacent sagittal slices. A_{ap} was calculated as the sum of two surface areas computed from ROIs 1 and 3 of coronal slices (right and left portions) and two surface areas computed from ROIs 1 and 3 of sagittal slices (anterior and posterior portions); posteriorly, A_{ap} was not computed in front of the spine. In addition to these four areas, the surface area of two frontal triangles was included in the calculation of A_{ap}. These triangles were defined by the xiphoid marker and the most

Table 2. *Mean values of diaphragm lengths obtained with CT and MRI*

	Lung Volumes			
	RV	FRC	FRC+	TLC
		L_{di}, *cm*		
Coronal				
CT	62.9	59.9	51.5	44.9
MRI	62.1	58.9	50.8	45.0
Sagittal				
CT	45.4	42.3	35.2	29.9
MRI	44.4	40.2	33.8	29.4
		L_{ap}, *cm*		
Coronal				
CT	31.4	28.6	18.3	10.5
MRI	32.9	29.1	19.0	11.5
Sagittal				
CT	26.5	21.8	14.3	10.1
MRI	27.6	22.4	14.8	9.9
		L_{do}, *cm*		
Coronal				
CT	31.5	31.3	33.2	34.4
MRI	29.2	29.9	31.8	33.5
Sagittal				
CT	18.9	20.6	20.8	19.9
MRI	16.8	17.9	19.1	19.5

CT, computed tomography; MRI, magnetic resonance imaging; L_{di}, length of diaphragm; L_{ap}, length of zone of apposition; L_{do}, length of dome; RV, residual volume; FRC, functional residual capacity; FRC+, FRC plus one-half inspiratory capacity; TLC, total lung capacity.

Downloaded from www.physiology.org/journal/jappl by ${individualUser.givenNames} ${individualUser.surname} (095.085.069.063) on November 26, 2018.
Copyright © 1997 the American Physiological Society. All rights reserved.

cranial and most caudal points of the right and left ROI-1 adjacent to the marker.

RESULTS AND DISCUSSION

The procedure was well tolerated by the subjects. The duration of each acquisition varied according to the height of the subject and the lung volume studied; it ranged from 15 to 25 s. Table 2 gives average values of L_{di}, L_{ap}, and L_{do} obtained with MRI and spiral CT. In general, CT values were in close agreement with MRI values, with differences of <15%. When data obtained at all lung volumes were pooled, L_{do} in the coronal and sagittal planes and L_{di} in the sagittal plane were significantly greater with CT than with MRI ($P < 0.05$, paired *t*-test).

Figure 3 shows changes in A_{di}, A_{ap}, and A_{do} with changes in lung volume for the four subjects studied. A_{di} and A_{ap} decreased almost linearly as lung volume increased, whereas A_{do} increased; regression coefficients relating lung volume to A_{di}, A_{ap}, and A_{do} were >0.97 in all cases. The decrease in A_{di} and A_{ap} between RV and TLC averaged 32.7 and 59%, respectively, while the increase in A_{do} was 12.3%. These results are very similar to those found by Gauthier et al. (1).

Table 3 gives average values of A_{di}, A_{ap}, and A_{do} obtained with MRI and CT, and Fig. 4 shows individual values. Average values of A_{ap} and A_{di} obtained with CT were 17.1 and 7.5% smaller than those obtained with MRI ($P < 0.01$–0.001), but a large part of this difference resulted from a large discrepancy in the A_{ap} value obtained for *subject S4* (● in Fig. 4). Inappropriate positioning of the costal marker in either the previous (1) or the present study may partly explain this difference. In addition, the different values of A_{ap} (and A_{di}) found in the present study and the study of Gauthier et al. may be related to the method used to compute A_{ap}.

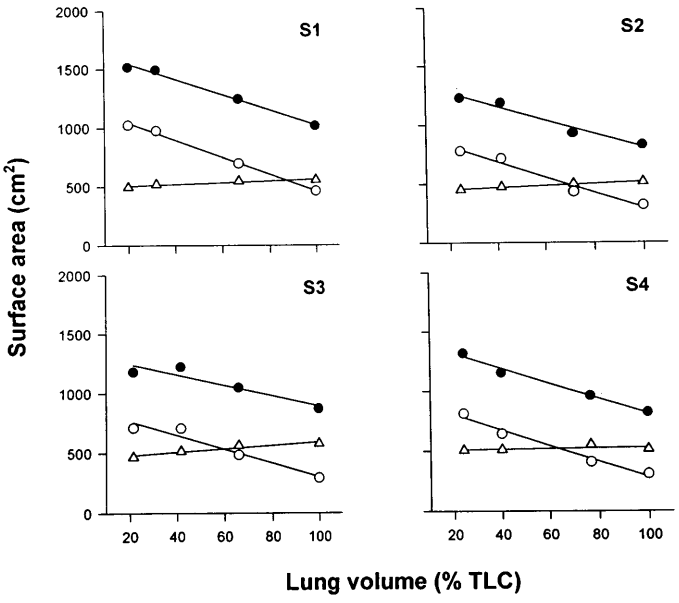

Fig. 3. Surface area-lung volume relationships for 4 individual subjects (S1–S4) [see Fig. 5 of Gauthier et al. (1) for comparison]. TLC, total lung capacity. ●, Total diaphragm area; ○, area of apposition; △, area of dome.

Table 3. *Mean values of diaphragm surface areas obtained with CT and MRI*

	Lung Volumes			
	RV	FRC	FRC+	TLC
		A_{di}, cm^2		
CT	1,312	1,265	1,045	883
MRI	1,461	1,351	1,130	925
		A_{ap}, cm^2		
CT	832	760	506	344
MRI	1,031	892	629	396
		A_{do}, cm^2		
CT	480	504	540	539
MRI	431	459	502	529

A_{di}, total diaphragm surface area; A_{ap}, surface area of zone of apposition; A_{do}, surface area of dome.

Because the area of apposition refers to the portion of costal diaphragm apposed to the rib cage, we considered that there was no muscle apposed to the spine, whereas Gauthier et al. did not interrupt A_{ap} in this region. For this particular part of the study, we believe that the present method of analysis provides more reliable data for A_{ap}.

In contrast to A_{di} and A_{ap}, A_{do} was on average 7.4% larger with CT than with MRI ($P < 0.001$). We suggest that this difference was due to the larger number of images reconstructed with CT. We used ~14 images in the coronal plane and ~20 images in the sagittal plane at each lung volume compared with 6 and 12 images for the reconstructions computed with MRI; reconstruc-

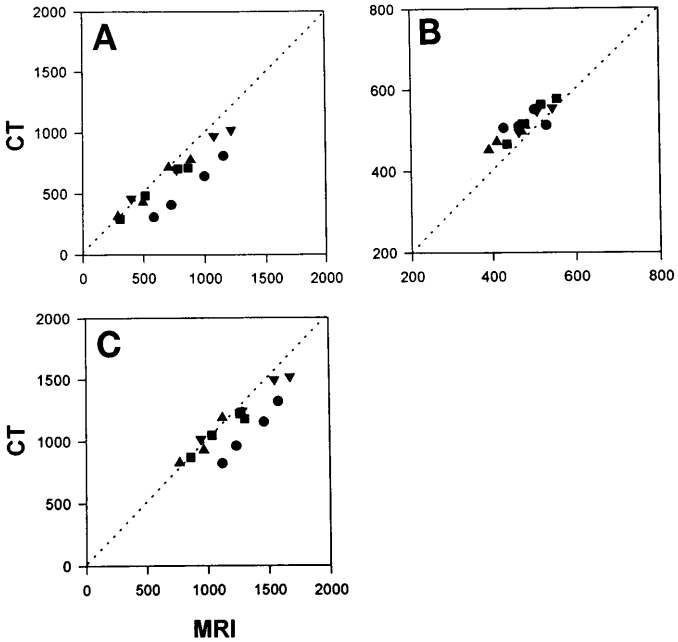

Fig. 4. Individual values of total diaphragm area (*A*), area of apposition (*B*), and area of dome (*C*) obtained with computed tomography (CT) and magnetic resonance imaging (MRI) in 4 subjects studied at 4 different lung volumes. Values are given in cm^2. Dotted lines, line of identity. ▼, *subject S1*; ▲ *subject S2*; ■, *subject S3*; ●, *subject S4*. See text for discussion.

Downloaded from www.physiology.org/journal/jappl by ${individualUser.givenNames} ${individualUser.surname} (095.085.069.063) on November 26, 2018.
Copyright © 1997 the American Physiological Society. All rights reserved.

tions obtained with a larger number of images are expected to provide a better fit of the spherical shape of the dome and hence larger values of A_{do}.

In conclusion, this study shows that satisfactory 3D reconstructions of the in vivo diaphragm may be obtained by using spiral CT. With a single acquisition of reasonable duration, this technique allows to reconstruct 20 coronal and 30 sagittal images at a given lung volume, allowing accurate measurements of muscle length, surface area, and shape.

Address for reprint requests: M. Estenne, Chest Service, Erasme Univ. Hospital, 808 Route de Lennik, B-1070 Brussels, Belgium.

Received 18 July 1996; accepted in final form 29 October 1996.

REFERENCES

1. **Gauthier, A. P., S. Verbanck, M. Estenne, C. Segebarth, P. T. Macklem, and M. Paiva.** Three-dimensional reconstruction of the in vivo human diaphragm at different lung volumes. *J. Appl. Physiol.* 76: 495–506, 1994.
2. **Ligier, Y., O. Ratib, M. Logean, and C. Girard.** Osiris: a medical image manipulation system. *Med. Diagn. Comput. J.* 11: 212–218, 1994.
3. **Paiva, M., S. Verbanck, M. Estenne, B. Poncelet, C. Segebarth, and P. T. Macklem.** Mechanical implications of in vivo human diaphragm shape. *J. Appl. Physiol.* 72: 1407–1412, 1992.
4. **Ratib, O., Y. Ligier, and J. R. Scherrer.** Digital image management, communication in medicine. *Comput. Med. Imaging Graphics* 18: 73–84, 1994.
5. **The Mathworks.** *Matlab, High-Performance Numeric Computation, Vizualization Software.* Natick, MA: Mathworks, 1992.

Downloaded from www.physiology.org/journal/jappl by ${individualUser.givenNames} ${individualUser.surname} (095.085.069.063) on November 26, 2018.
Copyright © 1997 the American Physiological Society. All rights reserved.